Thin Solid Films, *221* (1992) 127–131

Laser-assisted evaporation of high-quality narrow-gap thin films

S. V. Plyatsko, Yu. S. Gromovoj, G. E. Kostyunin, F. F. Sizov and V. P. Klad'ko
Institute of Semiconductors of the Academy of Sciences of the Ukraine, pr. Nauki, 45, Kiev-252650 (Ukra[redacted]

(Received December 11, 1991; revised April 30, 1992; accepted June 12, 1992)

Abstract

High-quality narrow-gap $Pb_{1-x}Sn_xTe$ ($0 \leqslant x \leqslant 1$) and $Hg_{0.74}Cd_{0.26}Te$ monocrystalline films were obtained on "cold" ($T \approx 290$–470 K) substrates by a laser-assisted evaporation method. It was proved that over a rather wide range of laser densities $W \approx (2$–$8) \times 10^4$ W cm^{-2} on the target (quasi-continuous regime of the CO_2 laser) and for substrate temperatures $T \approx 400$–500 K, good electrical characteristics (carrier concentrations $N_{77} \approx (3$–$30) \times 10^{16}$ cm^{-3}, carrier mobilities up to $\mu_{77} \approx (3-4) \times 10^4$ cm^2 V^{-1} s^{-1}) can be achieved which are comparable with those of the best single crystals obtained after long-duration thermal annealing at higher temperatures. The half-width of the Bragg diffraction profiles of the best films was in the range $\theta \approx 30''$–$50''$.

1. Introduction

Narrow-gap II–VI and IV–VI semiconductors are widely used for IR optoelectronics. To obtain the sharp metallurgical boundary needed for an abrupt interface, for example in heterojunctions or superlattices, low temperature deposition methods should be used. Up to now the lowest substrate temperatures used to obtain IV–VI monocrystalline layers and superlattices have been about 520 K (see for example ref. 1), leading to interdiffusion depths of about 10–30 Å.

For the growth of IV–VI thin layers and quantum-size structures, hot wall epitaxy (HWE), molecular beam epitaxy (MBE), liquid phase epitaxy (LPE) and vapour phase epitaxy (VPE) methods have mainly been used (see for example ref. 2). The electrical properties of the films obtained on heated substrates ($T \approx 650$–750 K) using VPE are not as good as required and the interdiffusion seems to be large. At lower temperatures, to exclude interdiffusion of the components, the crystalline quality of the layers is rather poor and they have poor electrical characteristics.

To produce IV–VI layers and structures of high quality, HWE and MBE methods have mainly been used (see for example refs. 1, 3–5). The quality of the individual layers of IV–VI semiconductors grown by either MBE or HWE is similar. In both methods IV–VI compounds are usually used as the source materials, rather than pure elements. The substrate temperatures are nearly the same ($T_{sub} \approx 520$–620 K [1, 3, 5]) in both methods. The growth rates for IV–VI semiconductors are about 1–3 μm h^{-1} for MBE and HWE, though for HWE they are normally a little higher. The great advantage of MBE is the possibility of *in situ* analysis of the quality and thickness of the layers.

In some papers [6, 7] methods of preparing IV–VI layers by laser-assisted evaporation of targets was discussed. Solid-state lasers were used. In this case the growth of $Pb_{1-x}Sn_xTe$ epitaxial layers in the Q-switched regime (neodymium–glass laser) proved to be possible on substrates cooled down to cryogenic temperatures ($T = 110$ K) [6]. The possibility of epitaxial growth under such conditions seems to be due to the high energy (approximately 10^3 eV) of ions present in the vapour–plasma flow. When implanting into the lattice they create condensation centres which are also the sources of layer structural defects. This seems to be the reason for the poor structural quality and electrical characteristics of PbSnTe layers.

High quality $Pb_{1-x}Cd_xSe$ layers with good electrical characteristics were obtained by laser assisted evaporation (free generation regime, neodymium–glass laser, $T_{sub} = 250$ K) [7].

2. Experimental details and discussion

In order to diminish the number of high energy particles in the vapour–plasma flow and possible interdiffusion processes, the quasi-continuous regime ($f \leqslant 10^3$ s^{-1}, where f is the modulation frequency of the laser beam) of target evaporation by the CO_2 laser was used [8]. The temperature of the (100) NaCl, KBr, NaF, KCl, (111) BaF_2 and (100) CdTe substrates was in the range $T = 293$–473 K. The laser power density (at $\hbar\omega = 0.118$ eV) used to obtain monocrystalline

0040-6090/92/$5.00

$Pb_{1-x}Sn_xTe$ layers was varied in the range $W = 3 \times 10^2 - 10^5$ W cm^{-2}.

2.1. Electrical characteristics of undoped films

It was found that the electrical properties of layers deposited onto the substrates mentioned above depend very much on the type of substrate and its orientation, and also on the laser power densities on the target. Table 1 lists the carrier concentrations and mobilities of PbTe films obtained on (100) KCl substrates (T_{sub} = 423 K) with the power density of the CO_2-laser on the target. The best electrical characteristics of $Pb_{1-x}Sn_xTe$ films were obtained with laser power densities in the range $W = (2-8) \times 10^4$ W cm^{-2}. With mobilities $\mu_{77} = 3 \times 10^2 - 4 \times 10^4$ cm^2 V^{-1} s^{-1} the carrier concentration of electrons and holes in the PbTe films varied in the range $N, P = 3 \times 10^{16} - 10^{19}$ cm^{-3} (see also Table 2). The electrical characteristics of $Pb_{1-x}Sn_xTe$ films with various molar fractions of tin are presented in Table 3.

The less the disagreement between the lattice constants a_0(PbTe) and a_0(sub) is, the better are the electrical properties of PbTe monocrystalline layers obtained. Moreover, the electrical properties of the PbTe layers are best (the lowest carrier concentrations and the highest carrier mobilities) when the sign of the quantity Δa_0 ($\Delta a_0 = (a_0(\text{PbTe}) - a_0(\text{sub}))/a_0(\text{PbTe})$) changes to negative values but $a_0(\text{PbTe}) \approx a_0(\text{sub})$. Table 2 gives the lattice constants and expansion coefficients of the cubic substrates used for PbTe film deposition.

It was found that by changing the laser power density on the target the concentration values in the films can be changed. It is also possible to change the conductiv-

TABLE 1. The dependence of carrier concentrations and their mobilities in PbTe films on (100) KCl substrates on the power densities on the PbTe target, $T_{sub} = 423$ K

Sample	W (W/cm^{-2})	Conductivity type	N, P (cm^{-3}) $T = 77$ K	μ_{77} (cm^2 V^{-1} s^{-1})	d (μm)
1	1.0×10^4	p	9.11×10^{18}	6.81×10^3	2.5
2	2.0×10^4	p	5.72×10^{18}	1.14×10^4	2.0
3	2.5×10^4	p	7.11×10^{17}	2.16×10^4	2.8
4	3.5×10^4	p	1.12×10^{17}	3.21×10^4	2.1
5	4.5×10^4	n	1.21×10^{17}	3.71×10^4	2.5
6	6.5×10^4	n	4.65×10^{17}	4.11×10^4	2.2
7	9.0×10^4	n	6.93×10^{18}	1.01×10^4	2.5

TABLE 2. Lattice constants of cubic substrates used for thin film deposition of PbTe by laser-assisted evaporation, $T_{sub} = 423$ K

Compound	a_0 (Å) $T = 300$ K	Expansion coefficient $\alpha_0(10^{-6}$ cm$^{-1})$ $T = 300$ K	$\Delta a_0/a_0$(%) PbTe	N, P (cm^{-3}) $T = 77$ K	μ_{77} (cm^2 V^{-1} s^{-1})	d (μm)
PbTe	6.4605	19.9	—	—	—	
KCl	6.2910	37.6	+2.62	$N = 5.38 \times 10^{17}$	1.2×10^4	3.5
KBr	6.599	44.6	−2.14	$N = 2.68 \times 10^{16}$	2.5×10^4	4.5
NaCl	5.6501	39.2	+12.54	$N = 1.9 \times 10^{18}$	1.0×10^4	1.0
NaF	4.628	33.1	+28.36	$P = 4.72 \times 10^{16}$	2.8×10^3	1.0

TABLE 3. Electrical characteristics of $Pb_{1-x}Sn_xTe$ films obtained by laser-assisted evaporation on different substates

Sample	Composition x	Conductivity type	N, P (cm^{-3}) $T = 77$ K	μ_{77} (cm^2 V^{-1} s^{-1})	d (μm)	Substrate	T_{sub} (K)	Power (W cm^2)
1	0.10	p	4.4×10^{17}	1.9×10^4	3.3	NaF	430	8×10^4
2	0.134	p	2.3×10^{17}	1.5×10^4	5.3	KCl	430	8×10^4
3	0.20	n	2.8×10^{18}	1.2×10^4	2.4	KCl	430	9×10^4
4	0.20	p	1.1×10^{19}	3.4×10^3	0.3	KCl	390	9×10^4
5	0.20	p	1.8×10^{18}	8.9×10^3	5.5	BaF_2	410	9×10^4
6	0.20	p	1.2×10^{17}	1.6×10^4	6.0	NaF	460	7×10^4
7	0.20	p	1.4×10^{17}	5.5×10^3	7.4	CdTe	420	6×10^4
8	1.0	p	3.1×10^{19}	1.2×10^3	1.4	KBr	425	1×10^5

ity type of the films by increasing the laser power density. For example, the change in sign of conductivity type of PbTe layers on KCl substrates takes place at $W \approx 4 \times 10^4$ W cm^2 ($T_{sub} = 423$ K).

Over a wide range of CO_2 power densities good electrical characteristics of $Pb_{1-x}Sn_xTe$ layers ($x = 0.2$) can be obtained which are comparable with the properties of the best PbSnTe single crystals obtained after long duration thermal treatment ($N_{77} \approx 10^{17}$ cm^{-3}, $\mu_{77} \approx 4 \times 10^4$ cm^2 V^{-1} s^{-1} [9, 10]).

2.2. Structural characteristics

The fairly good structural perfection of the layers obtained by laser-assisted evaporation was determined using transmittance electron microscopy (TEM) diffraction and X-ray reflection spectra. The TEM diffraction spots of $Pb_{1-x}Sn_xTe$ ($0 < x < 1$) layers indicate the high regularity of the lattice. As an example, Fig. 1 shows the TEM diffraction pattern of an SnTe film obtained on a (100) KCl substrate.

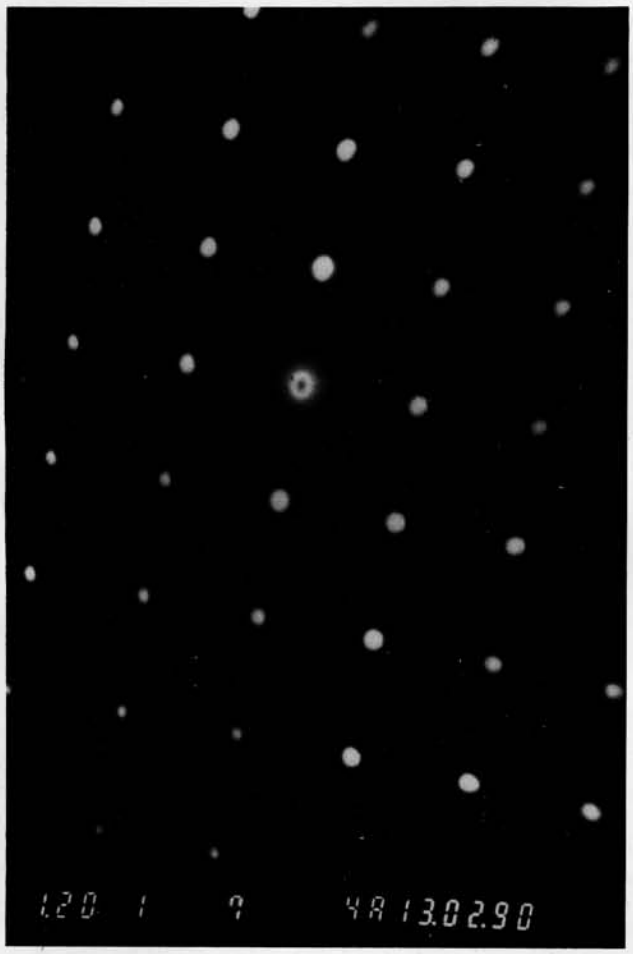

Fig. 1. Transmittance electron microscopy diffraction pattern of an SnTe film on a (100) KCl substrate, $T_{sub} = 373$ K.

Examination of the Bragg reflection spectra shows that the half-width of diffraction reflection lines for $Pb_{1-x}Sn_xTe$ layers on (100) KCl, KBr and (111) BaF_2 substrates reaches $\theta \approx 30''-50''$. Figure 2(a) shows diffractional reflection profiles about (1, 1, 1) reflections for two thin $Pb_{0.8}Sn_{0.2}Te$ films grown on BaF_2 substrates. Similar half-width values of diffraction reflection were obtained for $Pb_{1-x}Sn_xTe$ ($x = 0.2$) films with

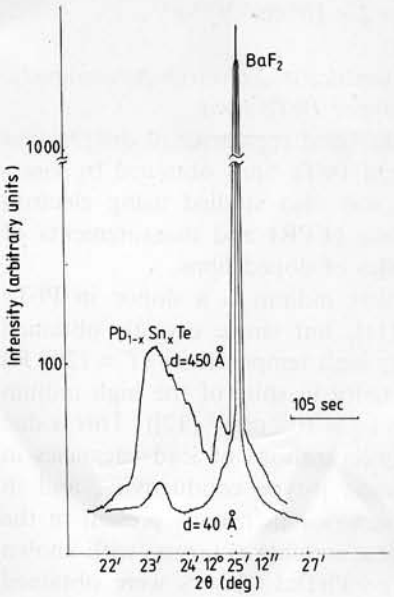

(a)

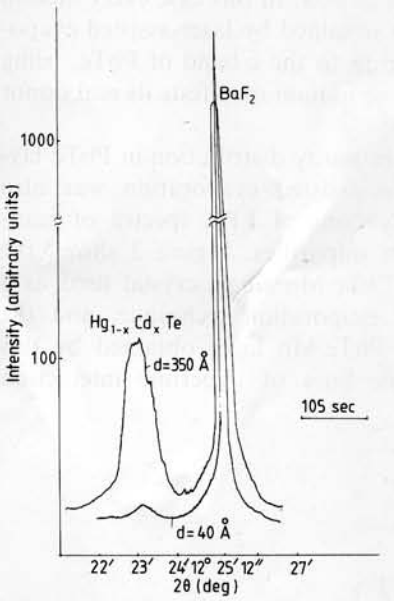

(b)

Fig. 2. Standard 2θ diffractometer scans of diffraction patterns around the [111] orientation of $Pb_{0.8}Sn_{0.2}Te$ and $Hg_{0.74}Cd_{0.26}Te$ films on (111) BaF_2 substrates, Cu $K\alpha_1$ radiation, $T_{sub} = 293$ K: (a) $Pb_{0.8}Sn_{0.2}Te$ films with $d = 450$ Å and $d = 40$ Å; (b) $Hg_{0.74}Cd_{0.26}Te$ films with $d = 350$ Å and $d = 30$ Å.

thicknesses up to 3 μm. Figure 2(b) shows the reflection profiles for two thin $Hg_{0.76}Cd_{0.24}Te$ films on BaF_2 substrates obtained by laser-assisted evaporation. Rather narrow halfwidths of the diffractional profiles are seen, characterizing the high crystalline quality of these samples. However, the electrical characteristics of these layers were not as good as those of $Pb_{1-x}Sn_xTe$ layers. For example, the concentration of electrons was about $10^{17}\,cm^{-3}$, which is a high value for $Hg_{1-x}Cd_xTe$ compounds, and their mobility did not exceed the value $\mu_{77} = 2 \times 10^3\,cm^2\,V^{-1}\,s^{-1}$.

2.3. Electrical characteristics and electron paramagnetic resonance spectra of doped PbTe films

The structural quality and regularity of distribution of ions in the lattice of PbTe films obtained by laser-assisted evaporation was also studied using electron paramagnetic resonance (EPR) and measurements of electrical chartacteristics of doped films.

It is well known that indium is a donor in PbTe crystals and layers [11], but single crystals obtained from the melt at fairly high temperatures ($T \approx 1200$ K) are of p-type conductivity in spite of the high indium concentrations ($N_{In} \approx 1.5 \times 10^{19}\,cm^{-3}$ [12]). This is due to the rather high concentrations of lead vacancies in the PbTe lattice causing p-type conductivity, and in part it is due to indium-rich inclusions present in the crystals [12]. Using these crystals as targets with known indium content, n-type PbTe:In layers were obtained with electron concentrations equal to the concentrations of indium in the targets. In this case every indium ion in the PbTe layer obtained by laser-assisted evaporation gives one electron to the c-band of PbTe, being in the state In^{3+}, and so indium manifests its real donor character.

The homogeneous impurity distribution in PbTe layers obtained by laser-assisted evaporation was also confirmed by investigations of EPR spectra of manganese and europium impurities. Figure 3 shows the EPR spectrum of a PbTe:Mn single crystal used as a target for the laser evaporation technique, and the EPR spectrum of a PbTe:Mn layer obtained by this method. Six isotropic lines of hyperfine interaction (HFI) with half-widths $\Delta H \approx 20$ Oe were observed in the lead telluride target. The rather large half-width of the six Mn^{2+} HFI lines are caused by the inhomogeneous distribution of Mn^{2+} ions in the PbTe lattice [13].

Superhyperfine interaction (SHFI) lines with half-width $\Delta H \approx 4$ Oe were previously observed in the EPR spectra of Mn^{2+} ions, allowing the position of Mn^{2+} in PbTe single crystals (Pb^{2+} sites) with "traces" of manganese to be determined [14], and also in laser-treated single crystal PbTe:Mn [13]. However, in these papers the ratio 1:4:1 between the satellite intensities of SHFI lines around the HFI lines, which proves random homogeneous distribution of Mn^{2+} ions interacting with tellurium nuclei of the first coordination sphere was not obtained. The 1:4:1 ratio for SHFI and HFI should be due to the random distribution of tellurium isotopes in the PbTe lattice approximately (82% of ^{126}Te have nuclei spin $I = 0$, and 7.1% of ^{125}Te and 0.87% of ^{123}Te have spin nuclei $I = 1/2$).

In PbTe laser-assisted deposited layers on KCl substrates the pronounced SHFI lines of the EPR spectra and also the ratio 1:6:1 between the SHFI and HFI lines obtained proves that these layers are high quality crystalline with homogeneous distribution of impurity ions.

A similar homogeneous distribution was obtained using EPR spectra for Eu^{2+} ions in PbTe layers.

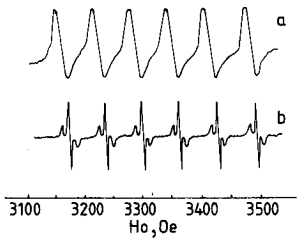

Fig. 3. The EPR spectra of (a) a PbTe:Mn target, $N_{Mn} = 10^{19}\,cm^{-3}$, and (b) a PbTe:Mn film, $d = 5$ μm, $T = 20$ K.

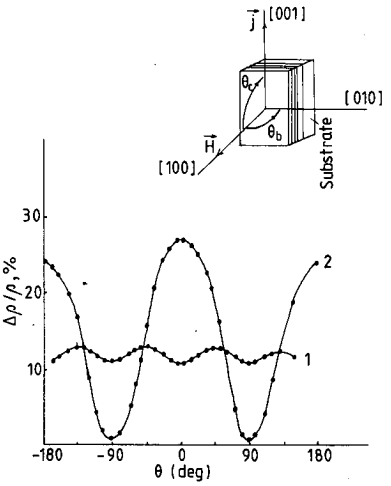

Fig. 4. The weak-field ($\mu H/c < 1$, where μ is the carrier mobility) magnetoresistance dependences (WFMR) in p-type $Pb_{0.8}Sn_{0.2}Te$ film (curve 1) and in a $PbTe/Pb_{0.8}Sn_{0.2}Te$ supperlattice (curve 2) ((PbSnTe) = (PbTe) = 220 Å, number of periods $n = 100$) on KCl substrates. In the film $d = 2.6$ μm, $P_{77} = 1.2 \times 10^{17}\,cm^{-3}$ m $\mu_{77} = 8.5 \times 10^3\,cm^2\,V^{-1}\,s^{-1}$. In the superlattice $P_{77} = 2.9 \times 10^{17}\,cm^{-3}$, $\mu_{77} = 9.8 \times 10^3\,cm^2\,V^{-1}\,s^{-1}$. The WFMR dependences were measured for B and C configurations (see the inset) but are shown only for the B configuration, as the data are similar for both the cases. Here $\boldsymbol{H}$ and $\boldsymbol{J}$ are the magnetic field and current directions.

3. Conclusion

The electrical and structural characteristics of $Pb_{1-x}Sn_xTe$ films obtained by laser-assisted evaporation using the quasi-continuous regime of a CO_2 laser, and also investigations of EPR spectra of Mn^{2+} and Eu^{2+} ions, proves the high quality of these films which can be used to obtain multiple layered structures including superlattices. Structures with rather high carrier mobilities (approximately $10^4\,cm^2\,V^{-1}\,s^{-1}$) were obtained and very pronounced quasi-two-dimensional conductivity in them was proved by angular dependences of the weak-field magnetoresistance (see Fig. 4) which is frequently used to test the two-dimensional character of free-carrier conductivity in superlattice structures [3, 4].

References

1 S. Shimomura, Y. Urakava, S. Takaoka, K. Murase, A. Ishida and H. Fujiyasu, *Superlattices Microstruct.*, *7* (1990) 5.

2 F. F. Sizov, *Acta Phys. Polon.*, *29* (1991) 83.

3 M. Kriechbaum, K. E. Ambrosh, E. J. Fantner, H. Clemens and G. Bauer, *Phys. Rev. B*, *30* (1984) 3394.

4 F. Sizov, M. Apatskaya, J. Gumenjuk-Sichevskaya, V. Tetyorkin and Y. Troyan, *Semicond. Sci. Technol.*, *5* (1990) 928.

5 D. L. Partin, *IEEE J. Quantum Electron.*, *24* (1988) 1716.

6 Yu. A. Biryunin, S. V. Gaponov, A. A. Gudkov, E. B. Klyenkov, B. M. Guskin and M. D. Strikovskiy, *Electronnaya Promishlennost*, (5–6) (1981) 110 (in Russian).

7 M. I. Baleva, M. H. Maksimov, S. M. Metev and M. S. Sendova, *J. Mater. Sci. Lett.*, *5* (1986) 533.

8 S. V. Plyatsko, Yu. S. Gromovoj and F. F. Sizov, *Infrared Phys.*, *31* (1991) 173.

9 Yu. I. Ravich, B. A. Efimova and I. A. Smirnov, *Semiconducting Lead Chalcogenides*, Plenum, New York, 1970.

10 A. Kh. Abrikosov and L. E. Shelimova, *Semiconductor Materials Based on IV–VI Compounds*, Nauka, Moscow, 1970, (in Russian).

11 V. I. Kaidanov and Yu. I. Ravich, *Usp. Fiz. Nauk*, *145* (1985) 51 (in Russian).

12. S. D. Darchuck, G. N. Panin, S. V. Plyatsko, F. F. Sizov and E. B. Yakimov, *J. Phys. Chem. Solids*, *15* (1990) 1333.

13. Yu. S. Gromovoj, S. V. Plyatsko and F. F. Sizov, *Mater. Lett.*, *8* (1989) 495.

14. M. Bartkovski, P. J. Nordcoth and A. N. Reddoch, *Phys. Rev. B*, *34* (1986) 6506.